

# $H_\infty$ Controller Design and Implementation for Induction Motors

Ciro Attaianesi, (Member), Giuseppe Tomasso  
University of Cassino

Department of Automation, Electromagnetism, Computer Science and Industrial Mathematics  
via G. di Biasio, 43 - 03043 Cassino (FR), Italy

## Abstract

Field oriented control of an induction motor fed by a VSI is achieved by means of a state feedback static controller designed according the  $H_\infty$  control theory. Designing procedure is described in the paper. The performances of the control system are numerically analyzed and experimentally verified, also in order to prove the validity of the design procedure. The results confirm that good dynamic performances and high robustness to variations of system's parameter can be achieved by means of the proposed controller.

**Key words:** induction drives, robust control.

## 1. Introduction

Vectorial control techniques make possible to achieve very high dynamic performances with induction motor drives, provided that system parameters are well known [1]. Moreover, in such control systems, an observer is often used to estimate the state variables which are not directly measured. Therefore, the uncertainties which always affect the knowledge of the system parameters, and the noise included in the detected signals can detune the control, making worse the performances. A very powerful tool for the design of robust controllers is represented by  $H_\infty$  optimization control theory [2] - [4]. It guarantees high quality performances regarding to the dynamic and steady-state response and, also, robust stability.

In previous papers [5] - [8] the  $H_\infty$  control theory has been applied in order to perform speed or position control of dc drives. This paper deals with the design of a  $H_\infty$  state feedback controller for speed control of an induction motor drive. The first approaches to the subject has been presented in [9] and [10], but theoretical results were derived under particular assumptions on the torque vs. time trajectory, and were not supported by the indispensable experimental validation. In the paper these limitations are removed. In particular, simulation and experimental investigation are performed, in order to validate the designing procedure of the proposed controller and to analyze the achievable performances.

## 2. Controller design

Strictly speaking from a theoretical point of view, the  $H_\infty$  control theory can't be applied to induction motor because of intrinsic system non-linearity. But, by making the same assumptions which are at basis of field oriented control, a linear plant can be set up, and the  $H_\infty$  control theory can be

used in order to set up a state feedback controller for field oriented control of an induction motor. This means that reference is made to induction motors fed by VSI with fast current control loop. In this case, only rotor equation can be taken into account, achieving a great simplification in the dynamic model of the motor. In fact, in order to get a mathematical description of the plant according the above assumptions, only the following set of simultaneous equations has to be considered:

$$\begin{cases} T_r \frac{di_{mr}}{dt} + i_{mr} = i_{sd} \\ J \frac{d\omega}{dt} = m_e - m_L \end{cases} \quad (1)$$

where  $m_e$  is the electromagnetic torque given by:

$$m_e = \frac{3}{2} p L_m i_{mr} i_{sq} = k_m i_{mr} i_{sq}$$

with:

$i_{sd}, i_{sq}$	direct and quadrature components of stator current in rotor field coordinates;
$i_{mr}$	magnetizing current representing rotor flux;
$p$	pole pairs;
$\omega$	motor velocity;
$m_L$	load torque;
$J$	inertia;
$L_m$	air gap inductance;
$T_r$	rotor time constant.

Starting from (1) the design of the  $H_\infty$  controller can be achieved, assuming  $m_e$  and  $i_{sd}$  as control inputs, and introducing as state variables the error quantities for the controlled variables, that is the speed and the magnitude of the

rotor flux. Denoting with  $i_{mr}^*$  and  $\omega^*$  the reference values of  $i_{mr}$  and of the speed respectively, the error variables are given by:

$$e_\varphi = i_{mr}^* - i_{mr} \quad e_\omega = \omega^* - \omega$$

Moreover, in order to achieve a zero velocity and flux errors at steady-state, the following state variables have to be introduced in the system model:

$$\frac{dv}{dt} = e_\omega \quad \frac{d\eta}{dt} = e_\varphi$$

Therefore, the simultaneous equations to assume in order to design the controller is expressed by:

$$\begin{cases} \frac{de_\varphi}{dt} = -\frac{1}{T_r} e_\varphi + \frac{1}{T_r} i_{mr}^* + \frac{di_{mr}^*}{dt} - \frac{1}{T_r} i_{sd} \\ \frac{d\eta}{dt} = e_\varphi \\ \frac{de_\omega}{dt} = \frac{d\omega^*}{dt} + \frac{1}{J} m_L - \frac{1}{J} m_e \\ \frac{dv}{dt} = e_\omega \end{cases} \quad (3)$$

System (3) can be considered as resulting from two decoupled subsystems: the electrical one, formed by the first two equations, and the mechanical one, corresponding to the third and fourth equations. This circumstance leads to a great simplification in the design of the  $H_\infty$  controller, because the designing procedure can be separately applied to the two subsystems. In particular, by denoting with superscripts  $e$  and  $m$  matrices and vectors corresponding to the electrical and to the mechanical subsystems respectively, for the control inputs  $\mathbf{u}^e$ ,  $\mathbf{u}^m$  yields:

$$\mathbf{u}^e = \mathbf{K}^e \mathbf{x}^e \quad \mathbf{u}^m = \mathbf{K}^m \mathbf{x}^m$$

with:

$$\mathbf{u}^e = (i_{sd}) \quad \mathbf{u}^m = (m_e),$$

and where the state vectors  $\mathbf{x}^e$ ,  $\mathbf{x}^m$  and the control matrices  $\mathbf{K}^e$ ,  $\mathbf{K}^m$  are given by:

$$\mathbf{x}^e = \begin{pmatrix} e_\varphi \\ \eta \end{pmatrix} \quad \mathbf{x}^m = \begin{pmatrix} e_\omega \\ v \end{pmatrix}$$

$$\mathbf{K}^e = -\left(\mathbf{D}_1^{eT} \mathbf{D}_1^e\right)^{-1} \left(\mathbf{B}_1^{eT} \mathbf{X}^e + \mathbf{D}_1^{eT} \mathbf{C}_1^e\right)$$

$$\mathbf{K}^m = -\left(\mathbf{D}_1^{mT} \mathbf{D}_1^m\right)^{-1} \left(\mathbf{B}_1^{mT} \mathbf{X}^m + \mathbf{D}_1^{mT} \mathbf{C}_1^m\right).$$

$\mathbf{X}^e$ ,  $\mathbf{X}^m$  are symmetric and positive definite matrices which satisfies the Riccati's inequality:

$$(\mathbf{A} - \mathbf{B}_2 \mathbf{R}_1^{-1} \mathbf{D}_1^T \mathbf{C}_1)^T \mathbf{X} + \mathbf{X} (\mathbf{A} - \mathbf{B}_2 \mathbf{R}_1^{-1} \mathbf{D}_1^T \mathbf{C}_1) +$$

$$+ \mathbf{C}_1^T (\mathbf{I} - \mathbf{D}_1 \mathbf{R}_1^{-1} \mathbf{D}_1^T) \mathbf{C}_1 + \mathbf{X} \left( \frac{1}{\gamma^2} \mathbf{B}_1 \mathbf{B}_1^T - \mathbf{B}_2 \mathbf{R}_1^{-1} \mathbf{B}_2^T \right) \mathbf{X} \leq 0$$

with:

$$\mathbf{A}^e = \begin{pmatrix} -\frac{1}{T_r} & 0 \\ 1 & 0 \end{pmatrix} \quad \mathbf{A}^m = \begin{pmatrix} 0 & 0 \\ 1 & 0 \end{pmatrix}$$

$$\mathbf{B}_1^e = \begin{pmatrix} \frac{1}{T_r} & 1 \\ 0 & 0 \end{pmatrix} \quad \mathbf{B}_1^m = \begin{pmatrix} \frac{1}{J} & 1 \\ 0 & 0 \end{pmatrix}$$

$$\mathbf{B}_2^e = \begin{pmatrix} -\frac{1}{T_r} \\ 0 \end{pmatrix} \quad \mathbf{B}_2^m = \begin{pmatrix} -\frac{1}{J} \\ 0 \end{pmatrix}$$

$$\mathbf{C}_1^e = \begin{pmatrix} c_1^e & 0 \\ 0 & c_2^e \\ 0 & 0 \end{pmatrix} \quad \mathbf{C}_1^m = \begin{pmatrix} c_1^m & 0 \\ 0 & c_2^m \\ 0 & 0 \end{pmatrix}$$

$$\mathbf{D}_1^e = \begin{pmatrix} 0 \\ 0 \\ d_1^e \end{pmatrix} \quad \mathbf{D}_1^m = \begin{pmatrix} 0 \\ 0 \\ d_1^m \end{pmatrix}$$

and where  $\gamma$  is a real and positive number, which is as lower as higher is the capability of the controller to reject the effects of the disturbances on the controlled outputs:

$$\mathbf{z}^e = \mathbf{C}^e \mathbf{x}^e + \mathbf{D}^e \mathbf{u}^e$$

$$\mathbf{z}^m = \mathbf{C}^m \mathbf{x}^m + \mathbf{D}^m \mathbf{u}^m$$

As exogenous input vectors  $\mathbf{w}^e$ ,  $\mathbf{w}^m$  the following ones have been assumed:

$$\mathbf{w}^e = \begin{bmatrix} i_{mr}^* \\ \frac{di_{mr}^*}{dt} \\ dt \end{bmatrix} \quad \mathbf{w}^m = \begin{bmatrix} d\omega^* \\ dt \\ m_L \end{bmatrix}$$

The elements of the matrices  $\mathbf{C}^e$ ,  $\mathbf{C}^m$ ,  $\mathbf{D}_1^e$ ,  $\mathbf{D}_1^m$  are weighting constants, which have to be determined so that the desired performance specifications are achieved.

For the whole system it obviously yields:

$$\mathbf{u} = \mathbf{K} \mathbf{x}$$

with:

$$\mathbf{u} = \begin{bmatrix} \mathbf{u}^e \\ \mathbf{u}^m \end{bmatrix} \quad \mathbf{K} = \begin{bmatrix} \mathbf{K}^e & 0 \\ 0 & \mathbf{K}^m \end{bmatrix} \quad \mathbf{x} = \begin{bmatrix} \mathbf{x}^e \\ \mathbf{x}^m \end{bmatrix}$$

The reference value of the quadrature component  $i_{sq}^*$  of the stator current in the rotor field coordinates, to impose in the field oriented control scheme, can be evaluated by means of the relation:

$$i_{sq}^* = \frac{m^*}{k_{m^*} \hat{i}_{mr}} \quad (10)$$

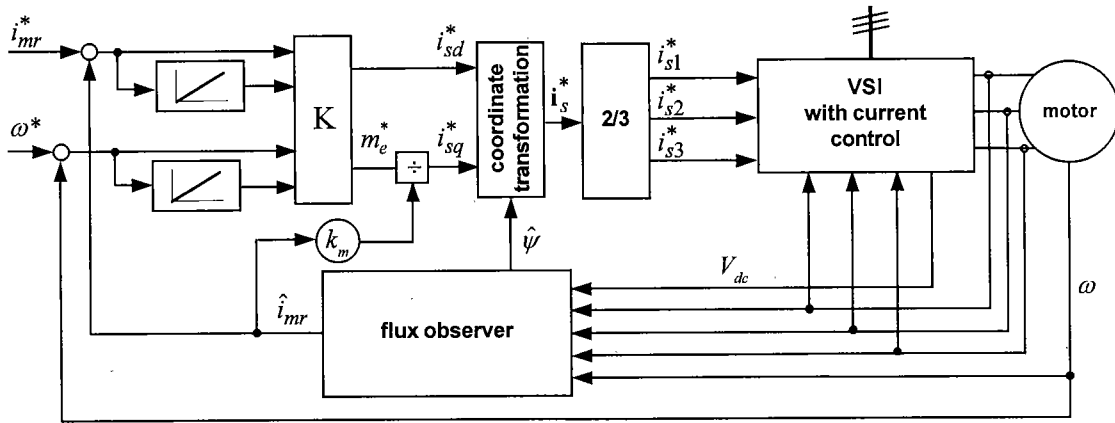


Fig.1. Schematic block diagram of the proposed control strategy.

where the caret ^ the observed quantities denotes.

### 3. Controller implementation

In fig.1 the schematic block diagram of the proposed control strategy is shown, where  $V_{dc}$  and  $\psi$  the dc link voltage and the argument of the space vector corresponding to the rotor flux respectively represent.

The experimental implementation of the proposed controller has been performed by means of a DSP-based full digital control system made by:

- Texas Instruments TMS320C40 50MHz DSP;
- optical incremental encoder for the measurement of the speed (20000 pulses per revolution, 12000 rpm maximum speed);
- Hall effect sensors for the acquisition of the stator currents (25 A rated current,  $\pm 0.5\%$  accuracy at 25°C, 1-2-3/1000 current ratio);
- Hall effect sensor for the acquisition of the dc bus voltage, (1000 V rated voltage,  $\pm 0.5\%$  accuracy at 25°C, 1/100 voltage ratio);
- A/D board with 32 multiplexed channels, 16 bit resolution, 3.5  $\mu$ s per channel acquisition time;
- digital I/O board (32 programmable I/o channels, 5 timer interrupts).

A sampling frequency of 15kHz has been imposed for measurement and control tasks. As observer a Luenberger full order

one [11] has been used.

### 4. Results

The controller design procedure above described has been applied to many motors of standard construction. A comparison between simulation and experimental results have been performed, in order to validate the controller design procedure above described. The possibility to have an effective simulation tool is very important for designing the  $H_\infty$  controller, because of the impossibility to determine the elements of the matrices **C** and **D** in explicit analytical form, as a function of the desired performances. For each motor different transient operations have been considered. In particular, the results achieved for the motor of tab.I and tab.II are presented in the following.

By imposing the following conditions in the  $H_\infty$  control problem for the motor of tab.I:

$$c_1^e = c_2^e = d_1^e = 1.0$$

$$c_1^m = c_2^m = d_1^m = 1.0$$

the following  $H_\infty$  controller is obtained:

$$\mathbf{K}^e = \begin{bmatrix} 6.0 & 0 \\ 0 & 10.8 \end{bmatrix} \quad \mathbf{K}^m = \begin{bmatrix} 1.9 & 0 \\ 0 & 2.4 \end{bmatrix}$$

Tab. I – Tested motor 1 data

power rating	750	[W]
rated voltage	380	[V]
pole pairs	2	
air gap inductance	657	[mH]
stator resistance	15.1	[ $\Omega$ ]
stator inductance	25.4	[mH]
rotor resistance referred to stator	9.4	[ $\Omega$ ]
rotor inductance referred to stator	17.0	[mH]

Tab. II – Tested motor 2 data

power rating	750	[W]
rated voltage	380	[V]
pole pairs	2	
air gap inductance	502	[mH]
stator resistance	12.1	[ $\Omega$ ]
stator inductance	22.4	[mH]
rotor resistance referred to stator	8.2	[ $\Omega$ ]
rotor inductance referred to stator	16.0	[mH]

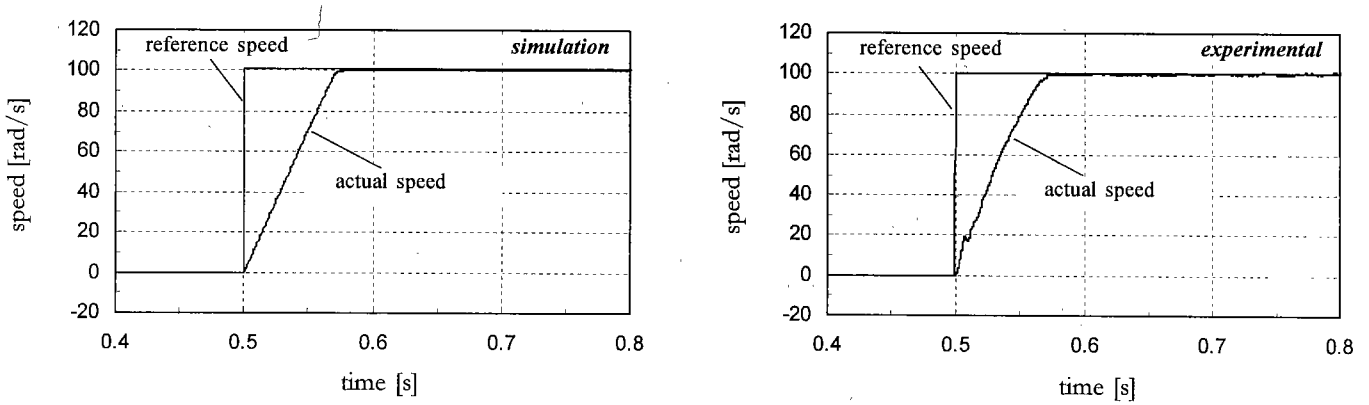


Fig. 2. Speed response of the motor 1 for a step variation of the speed command and with the rated load torque.

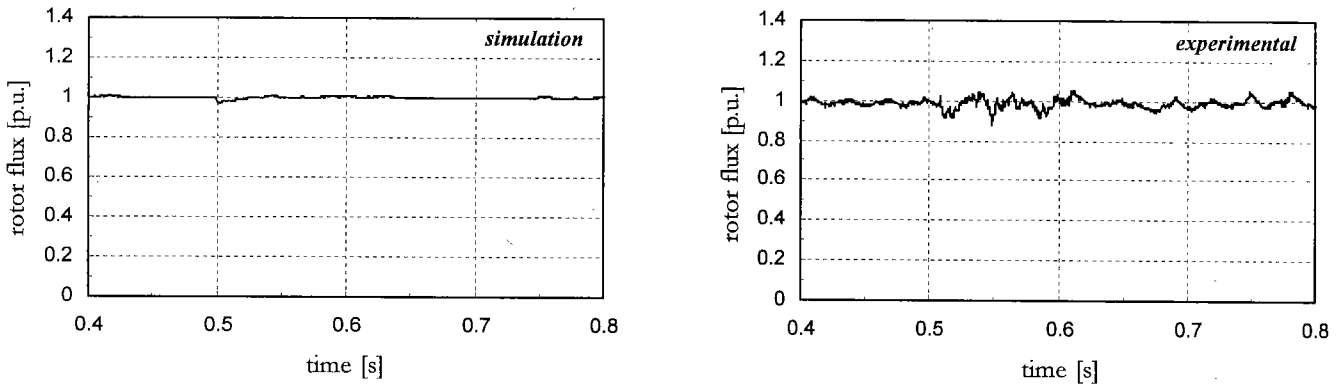


Fig. 3. Observed rotor flux response of the motor 1 for a step variation of the speed command and with the rated load torque.

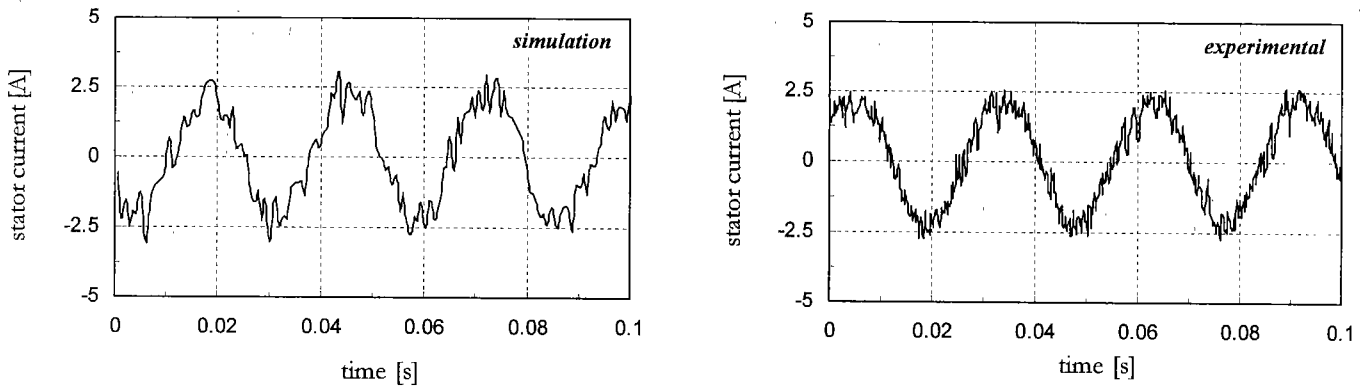


Fig. 4. Steady state stator current of the motor 1 with the rated load torque.

#### 4.1 Speed step response of the $H_\infty$ controller

A step variation from 0 to 100 rad/s of the reference speed command has been imposed. The rated torque has been imposed as load, while a saturation limit has been added to the control's output in order to keep the maximum value of the reference torque below 2.5 p.u. This factor just represents the ratio between the breakdown and the rated torque of the considered motors. The speed and flux responses, both in the simulation and in the experiment, are shown in figs. 2 and 3. The comparison of the two sets of figures confirms that the simulation produces results fully comparable with the experiment's ones. The experimental speed signal has been numerically filtered during the plotting in order to achieve a better comparison with the simulation. As

regards the flux response, it can be seen that no considerable variations from the imposed value occur, apart from a unavoidable noise on the experimental curve. Finally, in fig. 4 the steady state stator currents, again in the simulation and in the experiment, are shown.

A second test has been performed in order to compare the step up and the step down responses of the controlled motor. As a matter of fact, the  $H_\infty$  controller has been designed by considering, within the disturbances vector  $w$ , the reference speed and its derivative. Inspection of fig. 5, shows that the controller dynamic is practically independent on the reference profile imposed, being the step-up and step-down responses practically the same. The simulation curve has been omitted because it presents the same behaviour of the experimental one. The same results are achieved with different

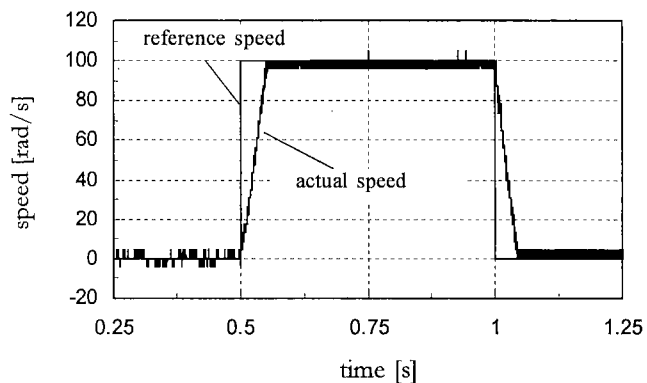


Fig. 5. **Experimental results:** speed response of motor 1 for a step up and a step down variation of the speed command and with the rated load torque.

step variations of the reference speed.

#### 4.2 Comparison with a traditional PI control

A field oriented control with traditional PI regulators as shown in fig. 6 has been considered in order to validate the proposed  $H_\infty$  controller design. The standard set-up of the field oriented control includes flux, torque and speed regulators in cascade topology. The design of the regulators has been performed in such a way as to achieve the best performance by the system and, at the same time, to make possible a proper comparison with the  $H_\infty$  controller. In particular, the gains of the PI flux regulator have been set to the same

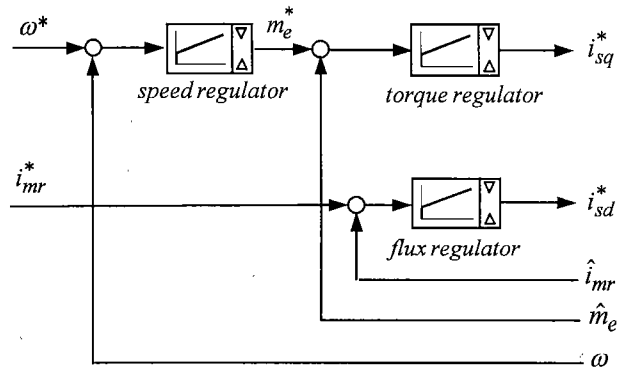


Fig. 6. Block diagram of a PI topology field oriented control.

values achieved by the  $H_\infty$  algorithm. As regards the torque and speed regulators, they have been tuned in such a way to achieve the best speed tracking behaviour within the saturation limit imposed. The gains and the sampling period for each loop and are listed in tab.III. The same operating conditions have been considered for  $H_\infty$  and PI control. In particular, the same saturation limits have been imposed at the regulators output. As reference speed command, a 400 rad/s<sup>2</sup> slope ramp has been imposed. This slope guarantees that the saturation limits are not exceeded when the rated torque is applied as load. Fig. 7 shows the simulation results, which are fully confirmed by the experiment. It can be seen that in PI control, only a partial decoupling of the flux response

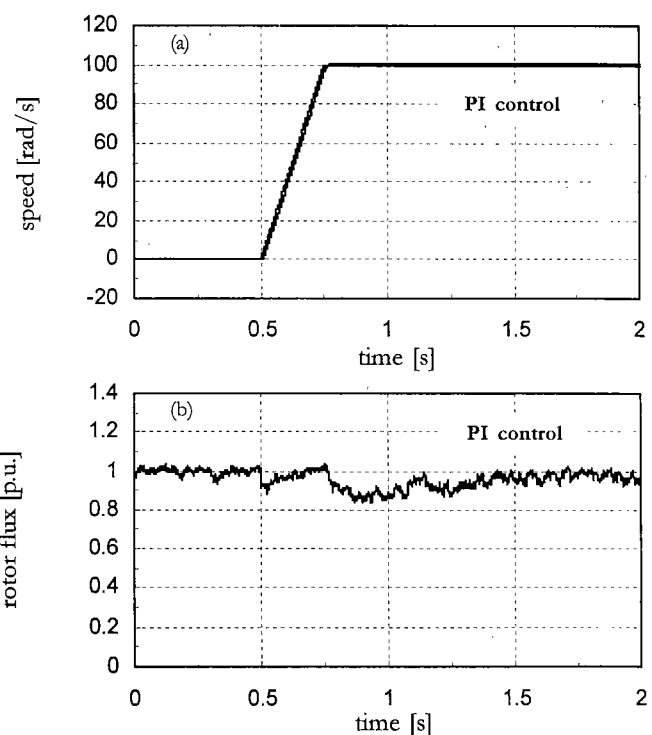
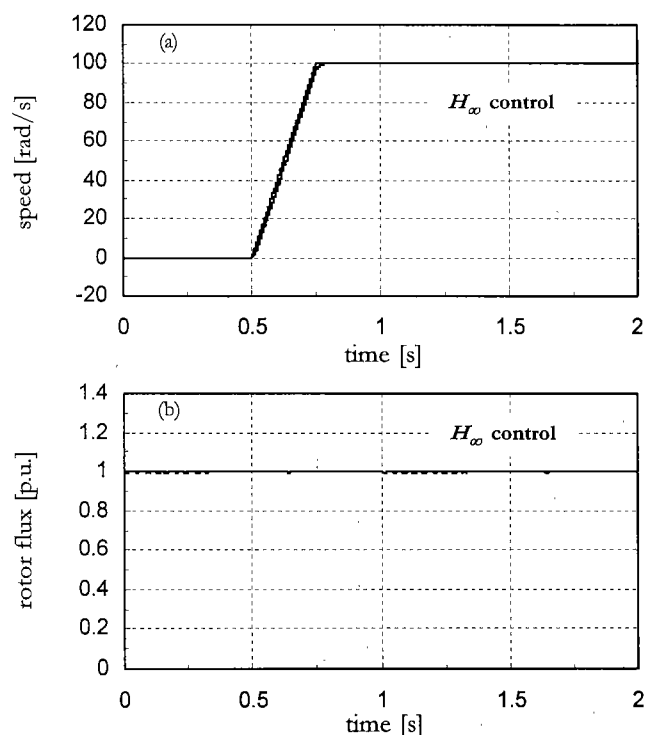


Fig. 7. **Simulation results:** comparison between  $H_\infty$  and PI control responses of the motor 1 for a ramp variation of the speed command.  
 (a) speed;  
 (b)observed rotor flux.

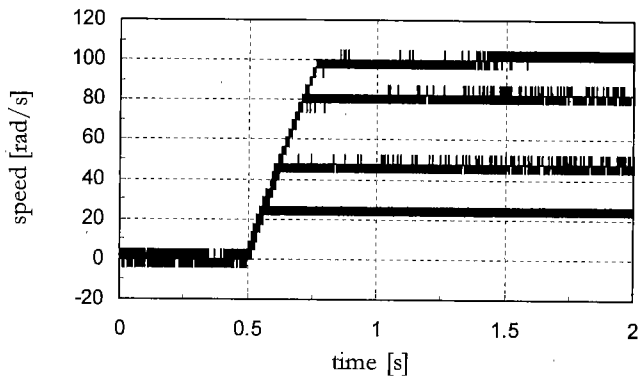


Fig. 8. *Experimental results:* speed response of motor 1 for a  $400 \text{ rad/s}^2$  slope ramp variation of the speed command and with the rated load torque.

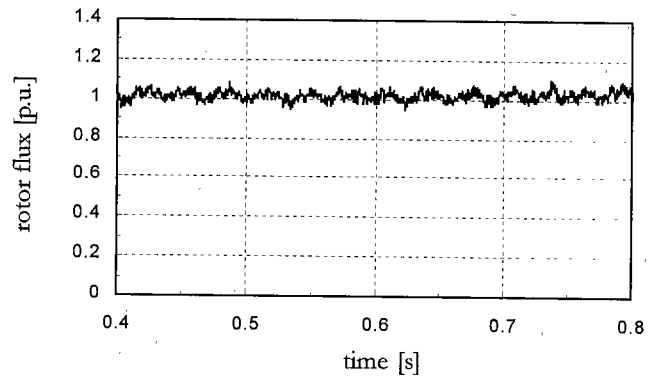


Fig. 9. *Experimental results:* observed rotor flux response of motor 1 for a  $400 \text{ rad/s}^2$  slope ramp variation of the speed command and with the rated load torque.

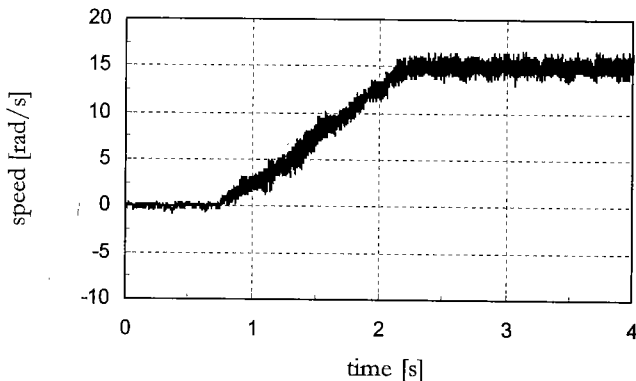


Fig. 10. *Experimental results:* speed response of motor 1 for a  $10 \text{ rad/s}^2$  slope ramp variation of the speed command and with the rated load torque.

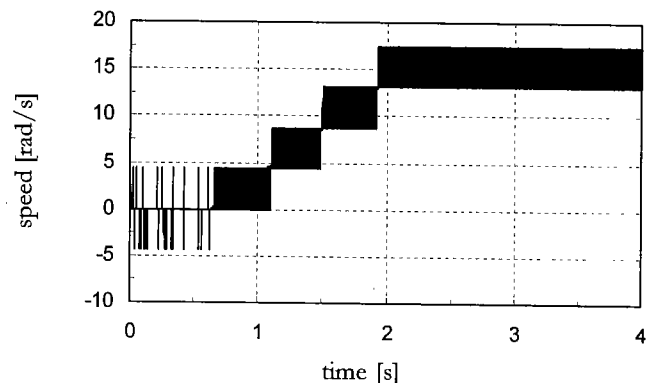


Fig. 11. *Experimental results:* speed response of motor 2 for a  $10 \text{ rad/s}^2$  slope ramp variation of the speed command and with the rated load torque, and a 100% increment of the whole inertia.

from the torque one is achieved. Instead, with the  $H_\infty$  controller, no appreciable variations of the flux occur. This behaviour becomes more marked if inertia and motor parameters variation is imposed.

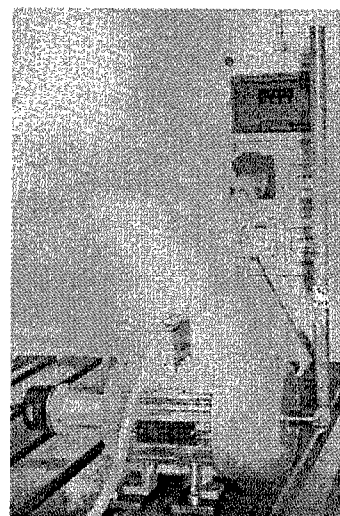
#### 4.3 Robustness against electrical and mechanical parameter variations

In order to test the robustness of the controller against the variations of the electric parameters of the motor, the same test of above has been performed by using the designed controller but controlling the motor of tab.II (motor 2), which has the same power rating, pole pairs and rated voltage of motor 1, but different electric parameters. No valuable differences have been detected.

Other tests have been performed on the same motors but changing the speed profile and the mechanical parameters. In particular, fig. 8 shows the speed transients of motor 1 achieved by applying different ramps as reference speed commands with the same slopes ( $400 \text{ rad/s}^2$ ) but different final values. Unlike fig.2, no numerical filtering has been applied to the speed signal. No overshoots or considerable tracking errors are present during the whole transient, confirming the good tracking propriety of the designed controller. Besides, in fig. 9 the observed rotor flux transient is

shown. Again, no considerable variations from the rated value are present.

The robustness of the  $H_\infty$  controller against simultaneous variations of inertia, electric parameters, and different measurement noise has been verified too. In particular, the same



*Iron bar parameters:*

length	0.42	m
weight	0.38	kg
inertia	0.05	$\text{kg m}^2$

Fig. 12. Particular of the assembly of the induction motor and the iron bar.

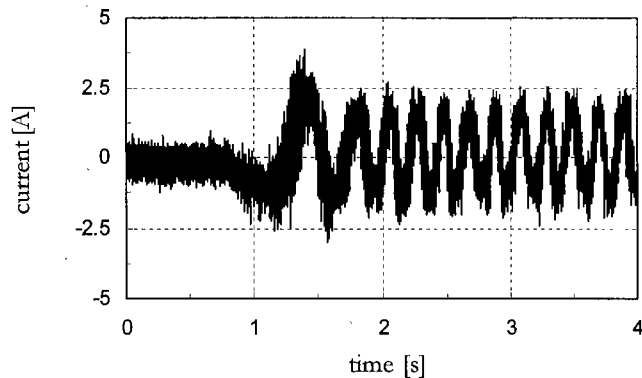
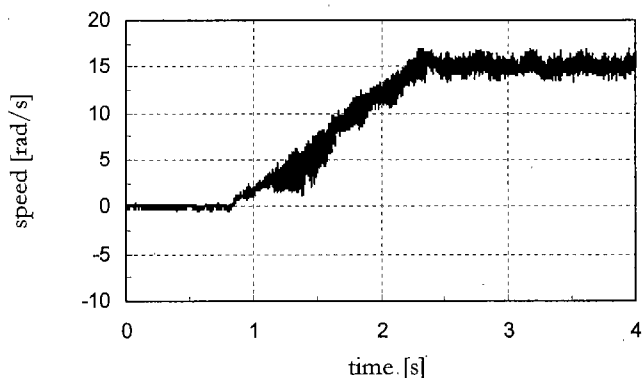


Fig. 13. **Experimental results:** speed response of the motor 1 for a 10 rad/s<sup>2</sup> slope ramp variation of the speed command and with the iron bar of fig.11 fitted in the motor shaft.

Fig. 14. **Experimental results:** current transient of the motor 1 for a 10 rad/s<sup>2</sup> slope ramp variation of the speed command and with the iron bar of fig.11 fitted in the motor shaft.

controller has been again used for controlling motor 2, but increasing of a 100% factor the system inertia, and using a different incremental encoder with 2000 pulses per revolution. The results achieved when a 10 rad/s<sup>2</sup> ramp with the rated load torque is imposed, are shown in figs. 10 and 11 where the plotting has been carried out by numerically filtering the speed signal. In particular, the mean value over 10 samples has been taken into account. Once more, the tracking of the reference signal results to be appreciable, in spite of the low value of the speed and the bigger relative speed error.

For the last test, an iron bar, has been fitted in the motor shaft, as shown in fig. 12. It gives rise to a considerable increment of the total system inertia (more then 400%) and it produces a position dependent load torque, with a maximum value of 0.25 p.u. The same ramp profile of the previous test has been imposed. In fig. 13, the experimental speed transient is depicted and it is almost the same achieved in the no load test. Besides, the system shows an optimum stability in spite of the particular load imposed. Fig. 14 shows, finally, the stator current during the speed transient.

**5. Conclusions**

In the paper, the  $H_\infty$  control theory has been used in order to design a state feedback static controller for field oriented control of induction motor. Several tests on different motors and in different operating conditions have been performed either with a simulation and with an experiment. Comparison with standard PI controller has been performed too. All the results achieved confirm that good dynamic performances and high robustness

to variations of system's parameter and exogenous disturbances can be achieved by means of the proposed controller.

(Manuscript received Jan. 31, 2000, revised Feb. 1, 2001)

**References**

- [1] Leonhard, W.: *Control of Electrical Drives*, Springer Verlag, 1990.
- [2] Doyle, J.C.; Glover, K.; Khargonekar, P.P.; Francis, B.A.: *State-space solutions to standard  $H_2$  and  $H_\infty$  control problems*, IEEE Trans. on Automatic Control, vol.34, n°8, 1989, pp.831-847.
- [3] Isidori, A.: *Nonlinear Control Systems*, Springer Verlag, 1990.
- [4] Stoorvogel, A.: *The  $H_\infty$  Control Problem*, Prentice Hall, 1992.
- [5] Mikami, Y.; Yamauchi, A.; Moran, A.; Hayase, M.: *Design of positioning  $H_\infty$  control system considering mechanical resonance and coulomb friction*, Proceedings of IPEC '95, vol.3, pp. 1429-1434, April 3-7, 1995, Yokohama, Japan.
- [6] Moran, A.; Mikami, Y.; Hayase, M.: *Analysis and design of  $H_\infty$  preview tracking control systems*, Proceedings of AMC'96, vol.2, pp.482-487, March 18-21, 1996, Mie University, Japan.
- [7] Attaianese, C.; Marongiu, I.; Perfetto, A.; Tomasso, G.:  *$H_\infty$  speed control of induction motor drives*, Proceedings of PEMC'98, vol.4, pp. 108-112, September 8-10, 1998, Prague, Czech Republic.
- [8] Attaianese, C.; Perfetto, A.; Tomasso, G.: *Robust Position Control of DC Drives by means of  $H_\infty$  Control*, IEE Proceedings on Electric Power Application, Vol.146, No. 4 July 1999.
- [9] Georges D., Canudas De Wit C.: *Non linear  $H_2$  and  $H_\infty$*

Tab. III – PI control: gains and sampling time of each loop

REGULATOR	PROPORTIONAL GAIN	INTEGRAL GAIN	SAMPLING TIME [s]
FLUX	6.0	10.8	10 <sup>-4</sup>
TORQUE	4.0	20.0	10 <sup>-4</sup>
SPEED	2.0	2.5	10 <sup>-3</sup>

---

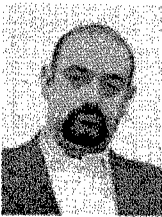
*optimal controllers for current-fed induction motors*, 1997 European Control Conference, Bruxelles, Belgium, 12-16 /07/ 1999, vol. 3, pp.1238-1243.

- [10] Canudas De Wit C., Ramirez J.: *Optimal torque control for current-fed induction motors*, IEEE Transactions on Automatic Control, May 1999, vol.44, pp.1084-1089.
- [11] Luenberger D. G.: *An introduction to observers*, IEEE Transactions on Automatic Control, 1971, vol.16, pp.596-602.



**Ciro Attaianese** was born in Naples, Italy, on March 5, 1959. He graduated in electric engineering from the University of Naples, in 1983. His employment experience include the Procter & Gamble Company. In 1988 he took the Ph.D. in electric engineering. Since 1999 he is Full Professor of Electrical Drives at the Faculty of Engineering of the University of Cassino. His main fields of interest

include electrical machines modeling, electrical drives and applications of microprocessors to their control. He is member of IEEE.



**Giuseppe Tomasso** was born in Cassino, Italy, on November 28, 1969. He graduated in Electrical Engineering from the University of Cassino, Italy, in 1994. In 1999 he took the Ph.D. in electrical engineering. At present he is researcher at the Faculty of Engineering of the University of Cassino. His research activities deals with microprocessor control of ac and dc drives, inverter modulation strategies.